

Magyarországi és görögországi tanulmányterületek morfortektonikai elemzése digitális terepmodellezéssel

(Digital terrain modelling for the morphotectonic analysis of study areas in Hungary and Greece)

G. JORDAN¹, G. CSILLAG¹ and B.M.L. MEIJNINGER²

1. *Geological Institute of Hungary (MÁFI), Budapest, Hungary*

2. *Vening Meinez Research School of Geodynamics, Faculty of Geosciences, Utrecht University, The Netherlands*

ABSTRACT

Based on the study of landforms related to faults, geomorphological characteristics were translated into mathematical and numerical algorithms in this study. Topographic features represented by digital elevation models of the test areas were extracted, described and interpreted in terms of structural geology and geomorphology. A sequential modelling scheme was developed and implemented to analyse two selected study sites, in Hungary and NW Greece on local and regional scales. Digital terrain analysis methods applied in the proposed way in this study could extract morphotectonic features from DEMs along known faults and they contributed to the tectonic interpretation of the study areas.

1. INTRODUCTION

Systematic digital tectonic geomorphology analysis is hampered by (1) the lack of such studies in literature, and (2) the non-uniform description and use of relevant digital methods in different fields of the Earth Sciences. Essentially identical methods are often used in these different fields with different names and for different purposes that makes their adoption to digital tectonic geomorphology difficult. Accordingly, available software designed for the specific needs of each field of study does in many cases not offer all the operations required for consistent digital terrain analysis. Geographic information system (GIS) software can easily perform most of the analyses but some procedures may be very difficult to implement. Digital analysis of the kind presented here requires the use of an integrated system of many analytical and software tools.

Digital tectonic geomorphology is the integration of three components: structural geology, geomorphology and digital terrain analysis (DTA) (Jordan & Csillag, 2001; Jordan & Csillag, 2003). There is, however, a gap between structural geology and DTA. The objective of this study is to provide case studies for local and regional scale application of DTA for morphotectonic investigations. In view of the great diversity of morphotectonic features (Keller & Pinter, 1996; Burbank and Anderson, 2001), only a limited selection of fault-related landforms is discussed. The emphasis of this study is on the application of digital data processing and detailed tectonic geomorphology interpretations of the presented examples are provided elsewhere (Jordan et al., 2003).

2. STUDY AREAS

2.1 Kali Basin, Hungary

The Kali Basin is located in the south-western part of the Balaton Highland in the Carpatho-Pannonian region (Trunko, 1995; Budai et al., 1999) (Figure 1.). The southern bordering hills are made up by folded Permian red sandstone. In the central and eastern parts, gently folded Triassic sediments are exposed. The majority of the basin is filled with horizontally bedded Tertiary clastic sediments. Late Miocene to Pliocene basaltic volcanics occur in the northern and western parts of the area (Figure 1.A). SE-verging reverse faults in the northern domain and folds in the southern part formed during the Cretaceous (Figure 1.A). Strike-slip faulting dominated in the region during the Miocene, and extensional tectonics characterised the latest Tertiary (Late Miocene and Pliocene). At present, the area is seismically inactive.

The specific objective in this study of the Kali Basin is the extraction and characterisation of morphological features associated with known faults on a local scale. A DEM of the Kali Basin was obtained from the national DTA-50 digital grid elevation database, initially produced via a third-order spline function to interpolate from an original dataset of 10 m contour lines. The horizontal resolution of the grid is 50x50 m and the vertical resolution is 1 m. Elevations above sea level are given as integers in meters.

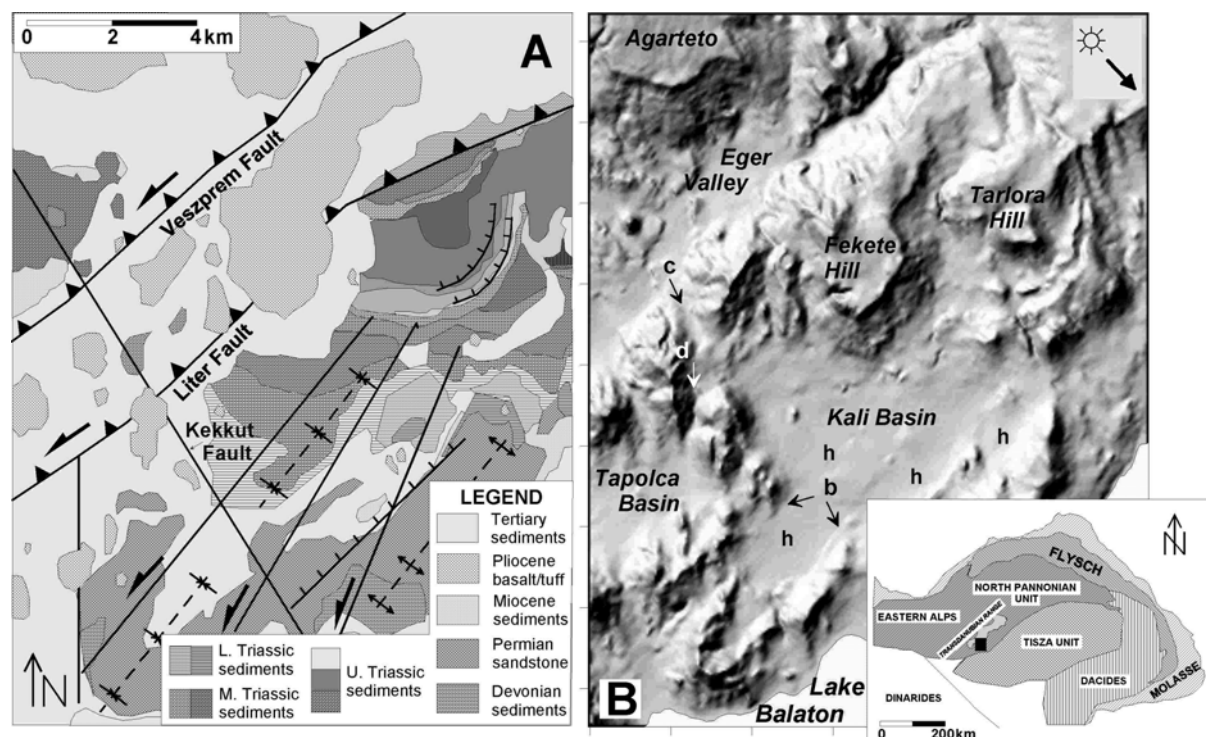


Figure 1. Kali basin study area. A. Geological map. Fault lines and fold axes indicated in geological maps are shown. B. Shaded relief model (6x vertical exaggeration). Solid arrow indicates illumination direction. Letters highlight specific features. Inset: location of the study area in the Pannonian Basin, Hungary (solid rectangle). See text for details.

2.2 North-western Greece

A second case study was carried out in north-western Greece, which exposes a NW-SE striking nappe pile (Figure 2.A) associated with African-Eurasian convergence in the course of the Late Mesozoic and Tertiary. The nappes themselves are internally highly folded and thrust. The age of nappe emplacement becomes progressively younger from east to west, subdivided in the (pre-)Apulian zone (autochthon) at the base of the tectonostratigraphy, overlaid by the Ionian zone, the Tripolitza zone, and the Pindos zone (Aubouin, 1957;

Bonneau, 1984) (Figure 2.A). Each of these zones consists of a Mesozoic to Lower Tertiary sequence of predominantly carbonates, overlaid by a Tertiary sequence of clays and turbiditic sandstones deposited in a foredeep environment (flysch) (IGRS-IFP, 1966). The Pindos zone was overthrust in the course of the Eocene by a complicated Jurassic to Early Eocene nappe stack of carbonates, an ophiolitic sequence and metamorphic rocks (e.g. Jacobshagen, 1986), which for the sake of convenience is indicated as the “Upper Unit” in the map of Figure 2.A.

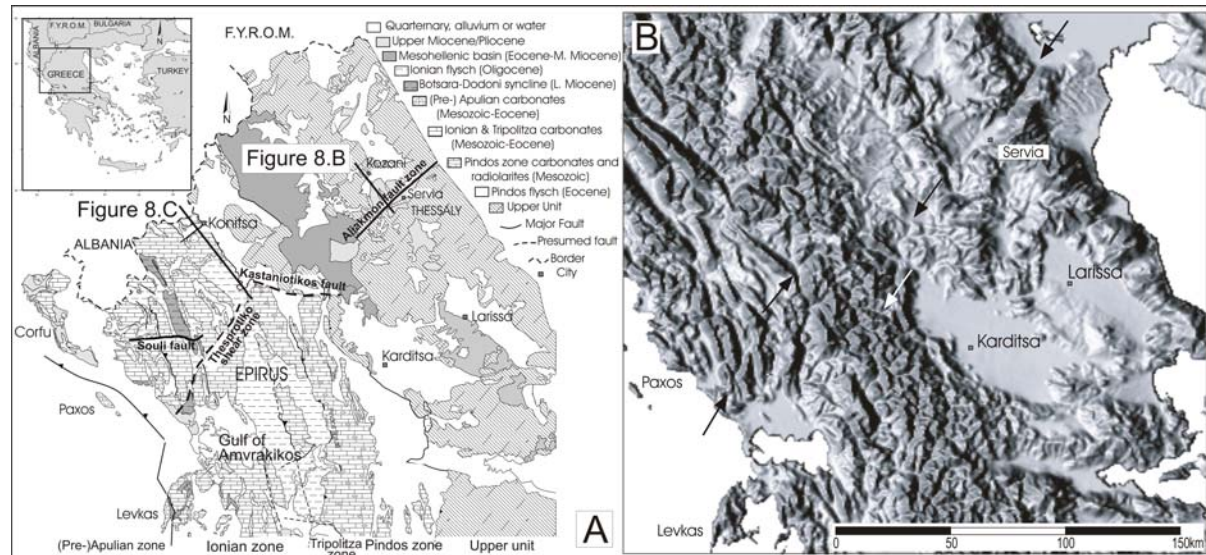


Figure 2. North-western Greece study area. A. Geologic map of north-western Greece with an inset indicating its position in Greece. B. Shaded relief model of original DEM (13x vertical exaggeration). Arrows indicate main lineaments in the NE-SW direction.

The nappe pile is cross-cut at high angles by a series of Late Tertiary extensional and strike-slip faults (Figure 2.A). Some of these have been described before and two zones will be identified here. The Late Mio-Pliocene and still-active Aliakmon fault zone in Thessaly (Figure 2.A) has been recognized as a major NE-SW trending NW-verging normal fault zone. The Servia fault, which belongs to the Aliakmon fault zone, bounds the Kozani Basin (Figure 2.A). It has an estimated vertical displacement of 2100 meters (Doutsos & Koukouvelas, 1998). The E-W trending Souli-fault in Epirus (Figure 2.A) is a normal fault with a component of left-lateral strike slip and has been active since some time after the Early Miocene until at least the Late Pleistocene (Boccaletti et al., 1997). A still-active NE-SW trending NW-verging normal fault is identified near Konitsa, forming the northern limit of the Timfi block (IGRS-IFP, 1966) (Figure 2.A), and a WNW-ESE trending, NNE-verging normal fault system, associated with the formation of the Gulf of Amvrakikos (Figure 2.A), is identified by Clews (1989). In the south-eastern part of north-western Greece, the intramontane basins of Karditsa and Larissa (Figure 2.A) are filled with Late Neogene to Holocene terrestrial deposits.

Based on the geologic map of IGRS-IFP (1966) and Bornovas & Rontogianni-Tsiabaou (1984) and are field observations, two fault zones are identified that have not been mentioned before in the literature: The Thesprotiko Fault Zone runs NE-SW across Epirus and displaces a syncline filled with Lower Miocene sediments in a right-lateral sense by 15-20 km (Figure 2.A). Its age is post-Early Miocene. It interferes with the Kastaniotikos fault zone (Skourlis & Doutsos, 2003), which is a WNW-ESE trending, north-verging normal fault zone, bringing the Upper Unit next to the Mesozoic carbonate sequence of the Pindos Zone (Figure 2.A) during an ill-defined time period after the Eocene.

In summary, the accentuated relief of north-western Greece is associated with a complex, but well-known geologic structure. It is therefore a very suitable area to test the applicability of DTA methods to identify tectonic features from geomorphology on regional scale.

A DEM of north-western Greece was obtained from the Global Land One-kilometre Base Elevation (GLOBE) model that has a 30 arc-second grid spacing and 1 meter vertical resolution. The DTA of the DEM of north-western Greece was carried out in combination with regional-size remote sensing (Landsat TM satellite images).

3. RESULTS AND DISCUSSION

3.1 Kali Basin, Hungary

The histogram of grid elevations shows systematic error in the DEM as spikes corresponding to the original contour lines at 10 m intervals (Jordan, 2003). A grey-scale elevation image shows a generally increasing elevation from SW to NE, indicating that the entire area is uniformly tilted towards the SW. Cross-sections across the basin in NE-SW direction also show the general dip of the area to the SW (Jordan et al., 2003).

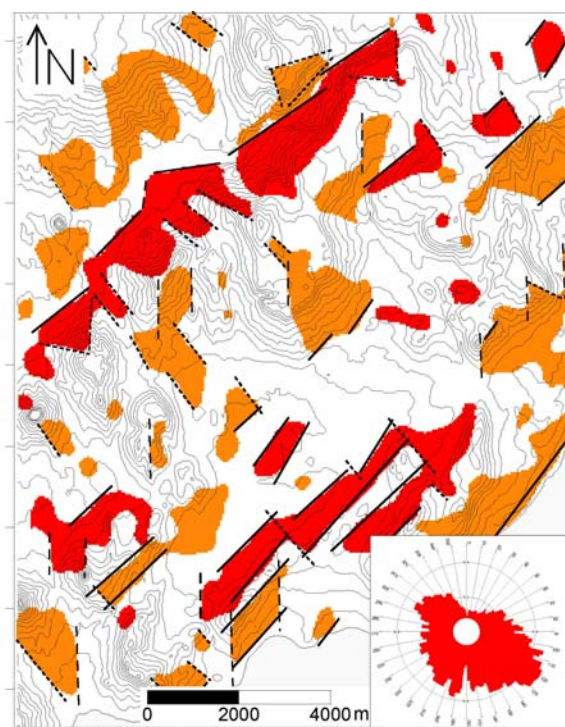


Figure 3. Classified aspect image after 11x11 majority filtering. Dark and light shaded areas have aspects between 290° and 340°, 110° and 160°, respectively. Lines are drawn to highlight edges of hill slopes. Solid line: NE-SW direction; dashed line: N-S direction; Dotted line: NW-SE direction. Elevation contours are also shown. Inset: rose diagram for aspect frequencies for slope > 1°.

Lineaments intersecting the entire basin in NE-SW direction are seen in the shaded relief image (b in Figure 1.B). The western boundary of the basin is marked by a series of volcanic cones aligning in a narrow N-S zone. N-S slope edges in the same direction are sharp (d in Figure 1.B). A third set of lineaments comprises NW-SE striking slope-breaks, and ridges and valleys crosscutting the study area (c in Figure 1.B). Six-time vertical DEM exaggeration reveals a number of closed depressions in the basin area (h in Figure 1.B). Note that closed depressions are artefacts resulting from the spline interpolation error inherent to the initial preparation of the DEM as mentioned above.

Due to large systematic errors in the aspect derived from the original spline DEM, aspect calculations discussed below used a new DEM interpolated by TIN from the original contour lines. Systematic error shown as peaks in the aspect histogram at values of 45° azimuth is due to numerical derivation over a rectangular grid. The aspect rose diagram, calculated only for hilly areas with slopes of more than 1° (Figure 2), displays two major directions: one facing SE (120°) and another pointing to the opposite direction (300°). The pronounced lack of land facets facing N and S suggests that E-W oriented morphological features are not characteristic for the area (compare to Figure 1). Based on the rose diagram (Figure 2), aspects were divided into two classes between 110° and 160°, and between 290° and 340°, respectively. The two aspect frequency peaks correspond to the flanks of the northern and southern hill ranges running in the NE-SW direction (Figure 3). Related areas are elongated and bounded by sharp linear edges. Slopes of uniform aspect commonly have N-S and NW-SE edges, suggesting possibly tectonic control on morphology.

Uniform slope is expected where contour lines are equidistant in the original map. On the basis of cumulative percentage area-slope curves (Jordan, 2003), areas were classified as plain, hilly and mountaineous where slopes are $\leq 1^\circ$, 1° - 3° and $>3^\circ$, respectively. A slope map displaying these classes shows sharp edges of the Kali Basin in the NE-SW, NW-SE and N-S directions.

The DEM, smoothed twice with a 3x3 moving average filter, was used as input for 2nd order derivatives. The resulting tangential curvature map displays valleys and ridges as white and black lines corresponding to positive and negative values, respectively (Jordan et al., 2003). The major NE-SW, NW-SE and N-S directions are apparent. Second-order derivatives in the X direction revealed prominent N-S linear features. The mixed second derivatives showed NE-SW and NW-SE running linear features representing valleys, ridges and slope-breaks (Jordan et al., 2003).

The regional tilt of the area was analysed by linear trend surface fitting to the whole basin area, to sub-areas, and to surface specific points. An overall dip of about 1° to the SE is apparent if the trend plane is fitted to the Kali Basin area (below 140 m a.s.l. and defined by slope $\leq 1^\circ$) only. The orientation obtained is consistent with the SW tilt found in elevation analysis. Note that the same tilt is found in field measurements on Tertiary seashore sediments (Csillag, 2003).

Autocorrelation analysis was performed after extraction of a linear trend and subsequent 5x5 average smoothing of the DEM in order to study lineation (anisotropy) and periodicity due to faulting or folding (Jordan, 2003). The main anisotropy direction resulting from this analysis is parallel to the main NE-SW lineation orientation found by the DTA procedures outlined above. A variogram in the E-W direction for the drainage-based artificial DEM displays a periodic shape, suggesting that the N-S running valleys are periodic with about 3000 m separation on average. Inspection of a periodogram calculated for the same DEM reveals that the large-scale valleys dominate the morphology with a marked NE-SW orientation (Jordan, 2003).

Lineaments defined by sharp grey-scale edges in the above images were digitised on screen (Figure 4.A). According to the rose diagram of lineaments (Figure 4.A), all linear features are oriented in one of the three main directions, i.e., 1) NE-SW, 2) N-S, and 3) NW-SE. Valleys, ridgelines and slope-breaks corresponding to these three directions crosscut the entire study area indicating a regional-size origin of these features. The three major orientations are consistent with the findings above. Since most of the valleys with these orientations crosscut

different rock types in the area they cannot be related to bedding only. Digitally extracted drainage network and segment orientations are shown in Figure 4.B. The three major orientations are consistent with the findings above. The E-W petal in the rose diagram is interpreted here as an error caused by drainage extraction from a rectangular grid, because grid-based drainage extraction is biased towards the four principal directions (Wilson and Gallant, 2000). The NW-SE petal is the longest although individual valley lines are shorter than in the other two directions. The low scatter of segments around these directions implies that related valley lines are well-defined.

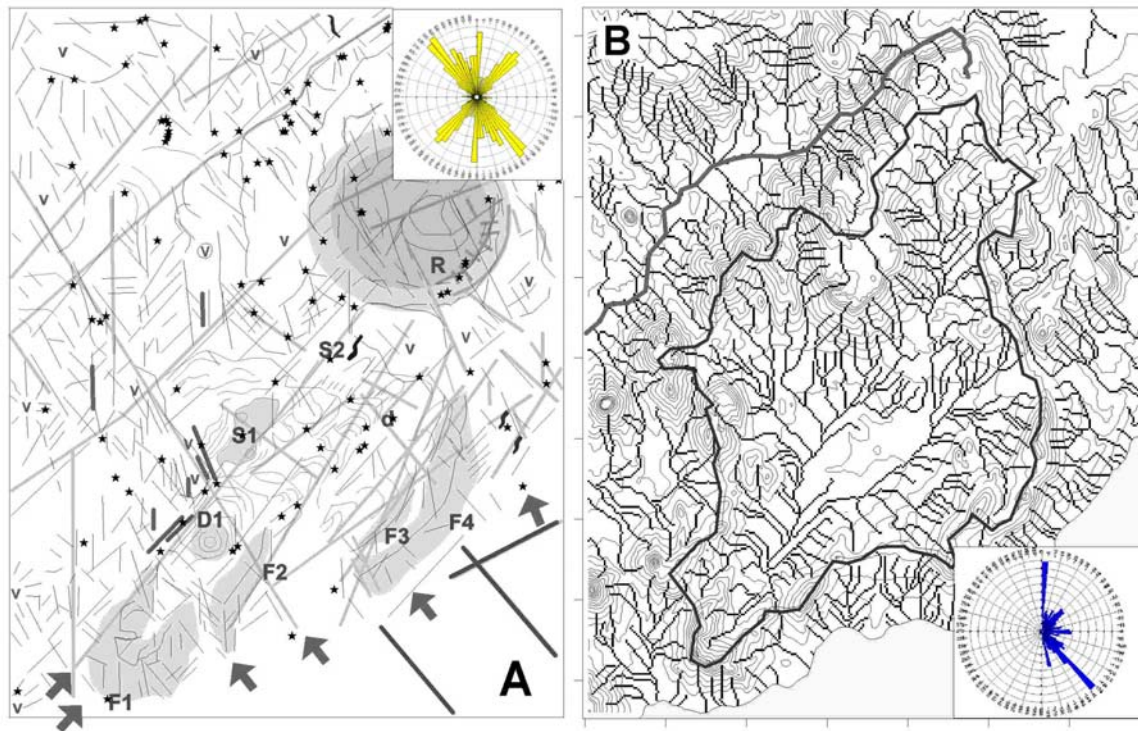


Figure 4. A. Lineament map. Black lines are line features (valleys, ridges and slope-breaks) digitised from terrain models. Grey polygons emphasise major morphological features. Thick light-grey lines show fracture lines shown in geological maps. Thick dark-grey lines show fracture lines recognised by other studies. Asterisks are springs. Large arrows show zones of springs. Key: D1: main depression; S1 and S2: S-shaped depressions; F1-F4: fold features; R: ring structure; d: asymmetric depressions; v: volcanic features. (For detailed analysis of these features see Jordan et al., 2003.) Inset: Rose diagram of lineaments. B. Watershed boundary of the Kali Basin (dark polygon) and valley lines for the study area defined by digital drainage extraction and watershed identification method. Valley line for the Eger Valley is highlighted (heavy grey line). Elevation contour lines are also overlaid. Inset: rose diagram for vectorised and smoothed channel segments with length > 300 m.

3.2 North-western Greece

For the digital tectonic geomorphology analysis of north-western Greece shaded relief models and differential geometry models such as aspect, slope and curvatures models were used. Morphological cross-sections were calculated perpendicular to significant fault lines. Satellite images were draped over the DEM to create three-dimensional views. Lineaments observed in shaded relief, aspect, slope and curvature models were manually digitised on the screen. Notwithstanding the relatively poor resolution of the DEM used, the results provide an acceptable regional morphotectonic view of the study area.

The histogram of the grid elevation shows a systematic error in the DEM as small spikes corresponding to 50 m intervals resulting from the primary grid cell processing of the

GLOBE model. Spikes at 10 m and at 110 m are related to the topographically low coastal regions in Epirus and Macedonia and to the Larissa and Karditsa basins in Thessaly, respectively (Figure 2.B).

The relief map shows high relief variability values in coastal regions and highly deformed areas in Epirus and along the borders of the Larissa and Karditsa basins.

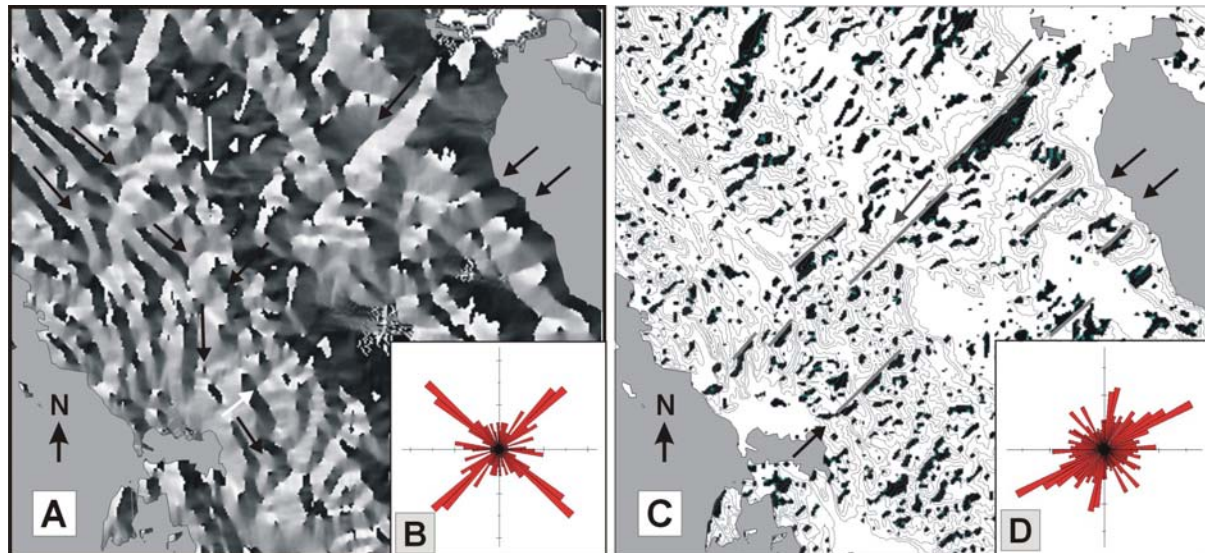


Figure 5. A. Grey-scale aspect image calculated from DEM smoothed with 7x7 moving average kernel. Arrows indicate main lineaments. B. Rose diagram of lineaments identified in the aspect model (n=125). C. Classified aspect image for angles between 280° and 350° after majority filtering. Dark and light tones show 3x3 and 5x5 majority filtering, respectively. Arrows and lines indicate main lineaments in the NE-SW direction. D. Rose diagram of lineaments identified in the satellite images (n=848).

Shaded relief models, calculated from DEMs smoothed by 3x3, 5x5, 7x7, 11x11 and 21x21 average filters, were displayed at 4 different illumination angles at 45° interval (Figure 2.B). The rose-diagram of lineaments identified in these shaded relief maps shows a subtle trend to the north and east, whilst there are few lineaments with NE-SW to WSW-ENE orientations.

A lineament map of the aspect analysis was constructed on the basis of the presence of fault facets, ridge cut-offs and uniform dips of hill slopes (Figure 5). Aspect maps were calculated from a DEM smoothed with a 7x7 average filter. Aspect angles were classed in 45° intervals and the classified aspect maps were subsequently filtered with a 5x5 pixel majority matrix to reduce noise and increase interpretability. For example, Figure 5.C illustrates an overlay map of two classified aspect images for the angles between 280° and 350°, one of which was filtered with a 3x3 majority matrix and the other with a 5x5 majority matrix. Figure 5.C illustrates the differences obtained when using different majority filters, and shows that the choice of majority filter to obtain an optimal result is a matter of trial and error. On the other hand, the map in Figure 5.C shows that corresponding areas are elongate and bounded by sharply defined linear edges in the NE-SW direction. In general, the resulting lineament map of the aspect analyses illustrates two pronounced lineament orientations trending NW-SE and NE-SW (Figure 5.B).

Linear patterns in slope and curvature maps, which could be interpreted as slope-breaks, were used as criteria to construct a lineament map. This construction involved two steps. Firstly, the slope map, calculated from a DEM smoothed with a 5x5 moving average filter, was

classified at $<4^\circ$, $4^\circ\text{-}8^\circ$, $9^\circ\text{-}11^\circ$ and $>12^\circ$ angles, these values being based on slope-breaks in the cumulative slope histogram. Next, the calculation of tangential curvature maps and profile curvature maps was performed on a DEM smoothed twice with a 5x5 moving average filter. The trend of the lineaments on the slope and curvature maps is, in general, NNW-SSE to NW-SE only with few numbers of lineaments in other directions. Most of the lineaments are located in Epirus and in the Olympos-Ossa mountain range to the east of Thessaly. The mixed second-order derivative map (Figure 8.A) illustrates a series of significant slope-breaks, which align along a series of NW-SE trending lineaments in Epirus.

The frequency (Figure 5.D) and length rose diagrams of the lineaments interpreted from satellite images illustrate a prominent NE-SW lineament orientation. Other but less prominent lineament orientations comprise NNE-SSW and NW to NNW lineament trends. There is also a fourth, less abundant set of lineaments in the E-W direction.

4. CONCLUSIONS

The use of DTA methods used in this study (1) yielded reproducible results, and (2) provided a quantitative description of morphotectonic landforms (Jordan and Csillag, 2003). Reproducibility is an improvement as compared with traditional morphological map analysis and visual image interpretation. Quantitative geometric characterisation of landforms based on DEM analysis is an advantage when compared with digital processing of remotely sensed images or analysis of grey-scale terrain images. Geometric terrain characterisation facilitates measurement of landforms and hence their comparison on a quantitative basis. The presented digital terrain analysis procedure thus provided a systematic and consistent framework for digital tectonic geomorphology.

From these data it could be inferred that the geomorphology of the Kali Basin was affected by tectonic processes, with most of the faults recognisable as regional morphological features in the regional-scale shaded relief model. The DTA of north-western Greece illustrated that major and minor structures could easily be identified in large areas of land and that it is, hence, a powerful tool to obtain a quick overview of the structure of an area.

ACKNOWLEDGEMENTS

Reinoud Vissers is gratefully thanked for critical reading of the manuscript. Thanks to Emőke Jocháné Edelényi and György Tóth of the Geological Institute of Hungary for providing facilities for the preparation of this paper.

REFERENCES

- Aubouin, J., 1957. Essai de corrélation stratigraphique de la Grèce occidentale. *Bull. Soc. Géol. France*, 7: 281-304.
- Boccaletti, M., Caputo, R., Mountrakis, D., Pavlides, S. and Zouros, N., 1997. Paleoseismicity of the Souli Fault, Western Greece. *J. Geodyn.* 24: 117-127.
- Bonneau, M., 1984. Correlation of the Hellenic Nappes in the south-east Aegean and their tectonic reconstruction. In: Dixon, J.E. and Robertson, A.H.F. (eds.) *The Geological Evolution of the Eastern Mediterranean*. Geol. Soc. Lond., Spec. Pub. 17: 517-527.
- Bornovas, I. and Rontogianni-Tsiabaou, T., 1984. Geological map of Greece. 2nd edition, 1:500.000, Institute of Geology and Mining exploration, Athens.

- Budai, T., Csaszar, G., Csillag, G., Dudko, A., Koloszar, L., and Majoros, G., 1999. Geology of the Balaton Highland. Geological Institute of Hungary, Budapest. (in Hungarian with English summary).
- Burbank, D. W. and Anderson, R. S., 2001. Tectonic Geomorphology. Blackwell Science, Malden.
- Doutsos, T. and Koukouvelas, I., 1998. Fractal analysis of normal faults in northwestern Aegean area, Greece. *Journal of Geodynamics*, Vol. 26, No. 2-4, 197-216.
- IGRS-IFP, 1966. Étude géologique de l'Épire (Grèce nord-occidentale). Editions Technip., Paris, 306 p.
- Jacobshagen, V., 1986. Geologie von Griechenland. Beiträge zur regionalen Geologie der Erde, 19. Bornträger, Berlin-Stuttgart. 363 p.
- Jordan, G., 2003. Morphometric analysis and tectonic interpretation of digital terrain data: A case study. *Earth Surface Processes and Landforms* 28: 807 - 822.
- Jordan, G. and Csillag, G., 2001. Digital terrain modelling for morphotectonic analysis: A GIS framework. In: H. Ohmori (ed), 2001. DEMS and Geomorphology. Special Publication of the Geographic Information Systems Association, 1: 60-61. Nihon University, Tokyo.
- Jordan, G. and Csillag, G., 2003. A GIS framework for morphotectonic analysis - A case study. *Proceedings, 4th European Congress on Regional Geoscientific Cartography and Information Systems, 17-20 June, 2003, Bologna, Italy. Proceedings, 2: 516-519. Regione Emilia-Romana, Servizio Geologico, Bologna.*
- Jordan, G., Csillag, G., Szucs, A. and Qvarfort, U., 2003. Application of digital terrain modelling and GIS methods for the morphotectonic investigation of the Kali Basin, Hungary. *Zeitschrift für Geomorphologie*, 47: 145-169.
- Keller, E., A. and Pinter, N., 1996. Active Tectonics: Earthquakes, Uplift and Landforms (New Jersey: Prentice Hall).
- Trunko, L., 1995. Geology of Hungary. Gebrüder Borntraegen, Berlin.
- Wilson, J. P. and Gallant, J. C., 2000. Terrain Analysis. Principles and Applications. London, John Wiley & Sons.